Effective field theories for QED bound states: Extending nonrelativistic QED to study retardation effects

Patrick Labelle*
Physics Department, McGill University, Montreal, Quebec, Canada H3A 2T8
and Physics Department, Champlain Regional College, Lennoxville, Quebec, Canada J1M 2A1†
(Received 15 October 1996; revised manuscript received 15 June 1998; published 5 October 1998)

Nonrelativistic QED bound states are difficult to study because of the presence of at least three widely different scales: the masses, three-momenta (p_i) and kinetic energies (K_i) of the constituents. Nonrelativistic QED (NRQED), an effective field theory developed by Caswell and Lepage, simplifies greatly bound state calculations by eliminating the masses as dynamical scales. As we demonstrate, NRQED diagrams involving only photons of energy $E_\gamma \simeq p_i$ contribute, in any calculation, to a unique order in α. This is not the case, however, for diagrams involving photons with energies $E_\gamma \simeq K_i$ (''retardation effects''), for which no simple counting counting rules can be given. We present an extension of NRQED in which the contribution of those ultra-soft photons can be isolated order by order in α. This is effectively accomplished by performing a multipole expansion of the NRQED vertices.
[S0556-2821(98)01121-7]

PACS number(s): 31.30.Jv, 11.10.St, 12.20.Ds, 36.10.Dr

I. INTRODUCTION

It is remarkable that the spectrum of the hydrogen atom is one of the first applications of quantum mechanics being taught and yet it is almost never mentioned in textbooks on quantum field theory and QED. Even when the problem of bound states is mentioned, it is made clear that it is a difficult subject and that, to quote Ref. [1], ''accurate predictions require some artistic gifts from the practitioner.''

The problem in studying bound states with relativistic quantum field theory is that the conventional perturbative expansion in the number of loops breaks down completely. The physical reason is the presence of energy scales absent from scattering theory. Indeed, the size of an atom made of two particles of charge $-e$ and Ze is of the order of the Bohr radius $\approx 1/(Z\mu\alpha)$ (where μ is the reduced mass) which, by the uncertainty principle, provides an additional energy scale $\approx Z\mu\alpha$. Because of this new energy scale, there is a region of the momentum integration in which the addition of loops will *not* result in additional factors of α. Moreover, if $Z \ll 137$ (condition to which we restrict ourselves in this paper), this energy scale is much smaller than the masses of the particles and the system is predominantly nonrelativistic, a simplification not taken advantage of in traditional approaches. In addition, a third energy scale, again vastly different from the previous two, is set by the particles kinetic energies $[\simeq (Z\mu\alpha)^2/m_i]$ and further complicates bound state calculations.

The problem is greatly simplified by using a Schrödinger theory corrected by the usual relativistic corrections obtained by performing a Foldy-Wouthuysen-Tani [2] transformation to the Dirac Lagrangian and expanding in powers of $\mathbf{p}/m$. These corrections include the Darwin interaction, the spin-orbit coupling, the relativistic corrections to the energy $[-\mathbf{p}^4/(8m^3)+\mathbf{p}^6/(16m^5]+\cdots$ and so on (from now on, it is this corrected theory that we will refer to as the ''Schrödinger theory''). The effects of these interactions can be computed by applying Rayleigh-Schrödinger perturbation theory using the Schrödinger wave functions as unperturbed states, a process familiar from elementary quantum mechanics. Calculations are much simpler in this framework because it takes advantage of the nonrelativistic nature of the problem.

However, such a theory is useless for high precision calculations. This is because it does not contain the physics corresponding to the high energy ($\mathbf{p} \simeq m$) modes of either the fermions *or* the photon. This has two consequences. The first one is the appearance of divergent expressions. These divergences show up in second order of perturbation theory (PT) as well as in first order of PT if sufficiently high order (in $1/m$) operators are considered; for example, the operator $\mathbf{p}^6/(16m^5)$ mentioned above is divergent when evaluated in first order of PT. These divergences are due to the fact that this theory reproduces faithfully QED only when the momenta probed by the interactions are much smaller than the electron mass. This condition is not satisfied in most interactions considered beyond first order PT, or when the operators contain sufficiently high powers of derivatives to probe the relativistic ($p \simeq m$) behavior of the wave functions.

The second consequence is the absence in the Schrödinger theory of operators corresponding to QED diagrams with photons of energies $\simeq m_e$, such as the process $e^-e^+ \to \gamma \to e^-e^+$ and the decay of of an electron-positron pair into an odd or even number of photons. These processes are clearly important; the first contributes to the lowest order hyperfine splitting in positronium, and the others cause the decay of the ortho (total spin $S=1$) and para ($S=0$) states of positronium.

*Email address: labelle@hep.physics.mcgill.ca
†Present address.

Let us emphasize again that these problems are due to the fact that, in a quantum field theory, the high energy modes cannot be simply discarded; they play an important role, even in processes involving only nonrelativistic external states.

Caswell and Lepage ([3,4]) have shown how to modify the Schrödinger theory to incorporate relativistic effects in a consistent and rigorous manner. They constructed an effective field theory (eft) that reproduces QED in the nonrelativistic regime ($\mathbf{p} \ll m_e$) and which they christened nonrelativistic QED (NRQED). Although NRQED has been around for more than ten years and have been used in high precision calculations in positronium and muonium ([3,5,6]), it is still little known, both by the atomic physics community and by the eft aficionados. Indeed, the Euler-Heisenberg Lagrangian, which describes the scattering of photons at energies much below the electron mass, is still the conventional example cited as an application of efts in the context of QED. However, the Euler-Heisenberg Lagrangian (which is a subset of the NRQED Lagrangian) has a range of applications quite limited which does not include, in contradistinction with NRQED, the important topic of bound state physics.

In the next section we will review the construction of NRQED. As any eft, NRQED contains an infinite number of interactions and is therefore nonrenormalizable. This is not a problem because an effective field theory is to be used within a restricted range of energy ($\mathbf{p} \ll m_e$ in the case of NRQED) so that only a finite number of interactions will contribute to any given process, at any given level of precision. Which interactions are to be kept for a given precision (in α) is dictated by counting rules which are an essential ingredient of any eft. The counting rules of NRQED are one of the focuses of this paper.

Clearly, NRQED can be applied to both low energy scattering and nonrelativistic bound states. In applications to bound states, the NRQED counting rules are more involved than in most eft's because of the presence, as noted above, of more than one dynamical scale in the theory: the fermions three-momentum $\simeq Z\mu\alpha$, and their kinetic energies $\simeq (Z\mu\alpha)^2/m_i$. For the sake of conciseness, from now on we will refer to these two scales as, respectively, the ''soft'' and ''ultra-soft'' energy scales, E_s and E_{us}. Because of the the presence of these two scales, there is, in general, no simple connection between an NRQED diagram and the order (in α) at which it contributes.

In this paper, we show how to disentangle the contributions from these two scales in such a way that each diagram will contribute to a unique order in α. The first step is well known and relies on time ordered (or ''old-fashioned'') perturbation theory together with the Coulomb gauge to separate the ''soft'' photons (with energy $E_\gamma \simeq E_s$) from the ''ultra-soft'' ones ($E_\gamma \simeq E_{us}$). The counting rules for the diagrams containing only soft photons are straightforward and a one-to-one correspondence between a diagram and the order of its contribution can be established. The diagrams with ultra-soft photons are more complicated; not only do they contribute to an infinite number of contributions of different order (in α), but in addition the lowest order is not given in terms of simple rules. This leads us to the second step in our separation of scales, which amounts to performing a multipole expansion of the vertices involving ultra-soft photons, leading to a new (infinite) set of interactions. This can be interpreted as defining an extension of NRQED which is more useful for dealing with ultra-soft photons and which we will call ''MQED'' (for ''multipole QED''). We will show that in MQED, diagrams containing ultra-soft photons contribute to a unique order in α, as given by new counting rules. In addition to having simple counting rules, MQED is better adapted to the study of processes involving ultra-soft photons such as the Lamb shift or the generation of certain types of logarithms. The example of the Lamb shift calculation can be found in another paper [7].

Our paper is divided as follows. In Sec. II we introduce NRQED and its Feynman rules, in the context of time ordered perturbation theory. In Sec. III we show how time ordered PT permits us to separate the contributions from soft and ultra-soft photons, and give the counting rules for diagrams containing only soft photons. In Sec. IV, we first illustrate the breakdown of the previous counting rules for diagrams containing ultra-soft photons. We then show how to incorporate the multipole expansion in the NRQED vertices, and how this leads to an extension of NRQED which we will call ''MQED'' for ''Multipole QED.'' In Sec. V we give the general MQED counting rules and some examples to illustrate their use.

II. NRQED

In principle, there are two ways of deriving an effective field theory if the underlying theory is know. Firstly, one can integrate out the modes of energies $\geqslant \Lambda_{phys}$ where Λ_{phys} is the energy below which the effective theory is to be used (we will keep the subscript *phys* to distinguish this Λ from the regulator cutoff to be introduced later on; in NRQED, $\Lambda_{phys} \simeq m$). In practice this is technically difficult to do or even impossible, as in the case of low energy QCD. The second method consists in writing down the most general effective field theory composed of the low energy fields and consistent with the symmetries of the underlying theory. The eft is not restricted by renormalizability and contains therefore an infinite number of operators, each accompanied by an independent coefficient. If the underlying theory is perturbative in the range of energy $E \leqslant \Lambda_{phys}$, then these coefficients can be computed, order by order in the loop expansion, by setting equal, or ''matching,'' some scattering process computed in both the underlying and the effective theories. In the case of low energy QCD, where such a matching is not possible, the coefficients must be determined phenomenologically and the usefulness of the eft is restricted by the wealth of data available.

For NRQED, we follow the second method which requires to first identify the low energy degrees of freedom and the relevant symmetries. There will be a field for the photon and one for each of the charged particles participating to the process under study such as the electron, the positron, the muon, proton, etc. Notice that the fermion fields correspond to two-components Pauli spinors. A particle and its associated antiparticle are independent fields in a nonrelativistic

field theory; they simply correspond to distinct particles of opposite charge. NRQED must obey the symmetries of low energy QED such as invariance under parity, Galilean and gauge invariance, etc. Lorentz invariance is not necessary except for the terms containing photon fields only.

It is convenient to decompose the NRQED Lagrangian in the following way:

$$\mathcal{L}_{\rm NRQED}=\mathcal{L}_{2-Fermi}+\mathcal{L}_{4-Fermi}+\mathcal{L}_{photon}+\cdots \tag{1}$$

where $\mathcal{L}_{2-Fermi}$ and $\mathcal{L}_{4-Fermi}$ are the interactions containing two and four fermions, respectively, and $\mathcal{L}_{photon}$ is the pure photon Lagrangian which includes the Euler-Heisenberg Lagrangian. We will not display the operators containing six or more fermions fields which, in all practical applications, can be ignored because their contribution is suppressed. The Lagrangian $\mathcal{L}_{2-Fermi}$ is given by

$$\begin{aligned}\mathcal{L}_{2-Fermi}=\psi^\dagger\Big(& iD_t+\frac{\mathbf{D}^2}{2m}+\frac{\mathbf{D}^4}{8m^3}\\ & +c_1\boldsymbol{\sigma}\cdot\mathbf{B}+c_2(\mathbf{D}\cdot\mathbf{E}-\mathbf{E}\cdot\mathbf{D})\\ & +c_3\boldsymbol{\sigma}\cdot(\mathbf{D}\times\mathbf{E}-\mathbf{E}\times\mathbf{D})+\ldots\Big)\psi\\ & +\text{same terms with } \psi\to\chi^\dagger\end{aligned} \tag{2}$$

where ψ and χ represent the (two-component) electron and positron fields, respectively. More precisely, $\psi^\dagger$ creates a two component electron field and $\chi^\dagger$ annihilates a two-component positron field. The parameter q represents the charge of the particle. Notice that in NRQED, a particle and its associated antiparticle differ only by their charge.

The first few terms of $\mathcal{L}_{4-Fermi}$ are given by

$$\begin{aligned}& c_4\psi^\dagger\boldsymbol{\sigma}(-i\sigma_2)(\chi^\dagger)^T\cdot\chi^T(i\sigma_2)\boldsymbol{\sigma}\psi+c_5\psi^\dagger(-i\sigma_2)(\chi^\dagger)^T\\ & \quad\times\chi^T(i\sigma_2)\psi+c_6(\psi^\dagger(-i\sigma_2)\boldsymbol{\sigma}\mathbf{D}^2\chi\cdot\chi^\dagger(i\sigma_2)\boldsymbol{\sigma}\psi+\text{H.c.})\\ & \quad+c_7\psi^\dagger\boldsymbol{\sigma}\psi\cdot\chi^\dagger\boldsymbol{\sigma}\chi+c_8\psi^\dagger\psi\chi^\dagger\chi+\cdots .\end{aligned} \tag{3}$$

The first three terms are only present when ψ and χ are associated with a particle and its antiparticle such as the electron and positron; they come from QED annihilation diagrams [the factors of σ_2 and the transpose operator T are necessary because we are using the same definition for both the particle and antiparticle spinors, see Eq. (15)].

As will become clear in our derivation of the counting rules, the Coulomb gauge is the most efficient gauge for the study of nonrelativistic systems. In this gauge, the first few terms of $\mathcal{L}_{photon}$ are [6]

$$\begin{aligned}& -\frac{1}{4}F_{\mu\nu}F^{\mu\nu}+c_9A^0(\mathbf{k})\frac{\mathbf{k}^4}{m^2}A^0(\mathbf{k})\\ & \quad -c_9A^i(k)\frac{\mathbf{k}^4}{m^2}A^i(k)\left(\delta_{ij}-\frac{k^ik^j}{\mathbf{k}^2}\right)+\cdots .\end{aligned} \tag{4}$$

Before discussing the calculation of the coefficients c_i, we will switch from the Lagrangian to the Hamiltonian. We do so because the counting rules in a nonrelativistic bound state are most easily derived in the context of time ordered (or ''old-fashioned'') perturbation theory (TOPT for short) and in TOPT one must work with the Hamiltonian rather than the Lagrangian. We remind the reader that, in contradistinction with covariant PT, in TOPT the vertices conserve only three-momenta and the virtual states are always on-shell. The total energy, however, is not conserved by the intermediate state so that, in this formalism, it is the violation of energy that characterizes the virtual state rather than the off-shellness of the particles, as in covariant PT.

Using $\mathbf{D}=i(\mathbf{p}-q\mathbf{A})$ and $D_t=\partial_t+iqA_0$, the NRQED Hamiltonian is given by

$$\begin{aligned}\mathcal{H}_{2-Fermi}=\psi^\dagger\Big(& \frac{\mathbf{p}^2}{2m}+qA_0-\frac{\mathbf{p}^4}{8m^3}-\frac{q}{2m}(\mathbf{p}'+\mathbf{p})\cdot\mathbf{A}+\frac{q^2}{2m}\mathbf{A}\cdot\mathbf{A}-ic_1\boldsymbol{\sigma}\cdot(\mathbf{k}\times\mathbf{A})-c_2\mathbf{k}^2A^0\\ & +2c_3\boldsymbol{\sigma}\cdot(\mathbf{p}'\times\mathbf{p})A^0-2qc_3\boldsymbol{\sigma}\cdot(\mathbf{k}_1\times\mathbf{A}(k_1))A^0(k_2)\\ & +c_3k^0\boldsymbol{\sigma}\cdot((\mathbf{p}'+\mathbf{p})\times\mathbf{A})+\cdots\Big)\psi(\mathbf{p})+\chi^\dagger\chi\ \text{ terms}\end{aligned} \tag{5}$$

$$\mathcal{H}_{4-Fermi}=-c_4\psi^\dagger\boldsymbol{\sigma}(-i\sigma_2)(\chi^\dagger)^T\cdot\chi^T(i\sigma_2)\boldsymbol{\sigma}\psi-c_5\psi^\dagger(-i\sigma_2)(\chi^\dagger)^T\chi^T(i\sigma_2)\psi+\cdots \tag{6}$$

$$\mathcal{H}_{photon}=\frac{1}{2}(\mathbf{E}^2+\mathbf{B}^2)-c_9A^0(\mathbf{k})\frac{\mathbf{k}^4}{m^2}A^0(\mathbf{k})+c_9A^i(k)\frac{\mathbf{k}^4}{m^2}A^i(k)\left(\delta_{ij}-\frac{k^ik^j}{\mathbf{k}^2}\right)+\cdots . \tag{7}$$

As explained previously, the coefficients are determined by computing some low energy scattering process in both QED and NRQED and matching the results. The coefficients of the operators in $\mathcal{H}_{2-Fermi}$ can be computed by considering the scattering of a charged particle off an external field (see Refs. [6] or [8] for an explicit matching). The coefficient

c_4 is obtained by matching the tree level QED annihilation diagram $e^+e^-\to\gamma\to e^+e^-$ to the NRQED interaction. The tree level contribution to c_5 comes from the QED diagram $e^+e^-\to\gamma\gamma\to e^+e^-$ and is therefore of order α^2. On the other hand, c_9 comes from the one-loop vacuum polarization. One finds

$$c_1=\frac{q}{2m}\quad c_2=\frac{q}{8m^2}$$

$$c_3=\frac{iq}{8m^2}\quad c_4=-\frac{\alpha\pi}{m^2}$$

$$c_5=\frac{\alpha^2}{m^2}(2-2\ln 2+i\pi)\quad c_9=\frac{\alpha}{15\pi}. \tag{8}$$

The imaginary part of c_5 corresponds, via the relation $\mathrm{Im(E)}=-\Gamma/2$, to the decay rate of positronium in a singlet ($S=0$) state, the quantum number carried by the corresponding operator.

Notice that the relation between the powers of α and the number of loops is broken in NRQED, since factors of the coupling constant arise from coupling to all photons whereas the eft contain only photons with momenta $|\mathbf{k}|\ll m$. For the same reason, the tree level matching, for example, involves NRQED tree diagrams, but may involve QED loop diagrams. By ''tree level matching'' we will mean matching involving tree level NRQED diagrams.

The one-loop matching modifies the values of the tree level coefficients so that we will, from now on, write the coefficients in the form

$$c_i\to c_i\delta_i \tag{9}$$

with $\delta_i=1+\mathcal{O}(\alpha)$. As in conventional renormalization, tree level as well as one-loop NRQED diagrams enter in the one-loop matching and this defines the $\mathcal{O}(\alpha)$ corrections to the NRQED parameters; the only difference with conventional renormalization is that the calculation is matched to a QED result instead of an experimental input. Because the one-loop NRQED integrals are divergent, they must be regularized. There are many possible regulators; one can use dimensional regularization or a simple cutoff Λ_R on the momentum integrations (which is permitted because NRQED breaks Lorentz invariance to start with). The NRQED coefficients defined by the matching are then cutoff dependent, i.e., they must be viewed as bare parameters. In contradistinction with QED, the divergent terms are not only logarithmic but power-law, $(\Lambda_R/m)^n$, as well. This cutoff dependence is of course canceled in any physical calculation, by invariance under the renormalization group. Obviously, one can also set $\Lambda_R=\Lambda_{phys}=m$ directly, but since the bare coefficients are then finite, this can be misleading if one is not careful about renormalizing the effective theory properly (for a more thorough discussion of this point, see [9]).

The one-loop matching of some of the coefficients appearing in Eq. (2) has been performed in Refs. [6] and [10] and the corresponding δ_i's appearing in Eq. (2) were found to be

$$\delta_1\equiv\delta_F=1+a_e+\mathcal{O}(\alpha^2)$$

$$\delta_2\equiv\delta_D=1+\frac{\alpha}{\pi}\frac{8}{3}\left[\ln\left(\frac{m}{2\Lambda_R}\right)+\frac{11}{24}\right]+2a_e+\mathcal{O}(\alpha^2)$$

$$\delta_3\equiv\delta_S=1+2a_e+\mathcal{O}(\alpha^2)$$

$$\delta_4\equiv\delta_A=1-\frac{44\alpha}{9\pi} \tag{10}$$

where a_e is the electron anomalous magnetic moment which, to the order of interest, can be taken to be $\alpha/(2\pi)$. We have redefine our coefficients to follow the convention of [6] (but notice that our δ correspond to their coefficients c); the subscripts F, D, S and $4-F$ stand for Fermi, Darwin, spin-orbit and four-Fermi interaction, respectively.

We now turn to the task of writing a general form for the NRQED coefficients. Before doing so, we must address the issue of the photon mass, which provides an additional scale and has the potential of complicating our analysis. The photon mass does not appear in Eq. (10) but this might appear fortuitous. However, since any photon mass dependence is a sign of sensitivity to very low momenta and NRQED is designed to be equivalent to QED in this region of phase space, any infrared singularity in a QED diagram is also present in the corresponding NRQED diagram, so that it gets canceled in the matching. Therefore, in general, the NRQED bare coefficients do not depend on the photon mass, to any order in the matching. From this, it follows that the coefficients have the general structure

$$\begin{aligned}c_i(\Lambda_R,m_1,m_2)&=c_i^0\alpha^{n_i}\delta_i(\Lambda_R,m_1,m_2)\\&\equiv c_i^0\alpha^{n_i}\left(1+\sum_{l_i=1}^{\infty}\alpha^{l_i}\tilde{c}_i^{l_i}(\Lambda_R,m_1,m_2)\right)\end{aligned} \tag{11}$$

where c_i is now a generic symbol representing any NRQED coefficient and the l_i on the coefficients $\tilde{c}_i$ is an index, not an exponent. We have decomposed the lowest order term as a coefficient c_i^0 of order one times a factor α^{n_i} which is different for different operators. As an example, the Darwin interaction, which contains the factor c_1, has $n_1=1/2$ whereas the singlet annihilation operator, which contains c_5, has $n_5=2$. The index l_i indicates the number of loops used in the matching.

The coefficients $\tilde{c}$ contain, in general, finite pieces plus power-law terms as well as logarithms divergent terms. Notice that for a fixed l_i, there are, in principle, an infinite number of terms to calculate because there are an infinite number of l_i-loops NRQED Feynman diagrams, but only a finite number of interactions must be considered in any given calculation, as specified by the counting rules (which will also dictate the order at which the matching must be performed).

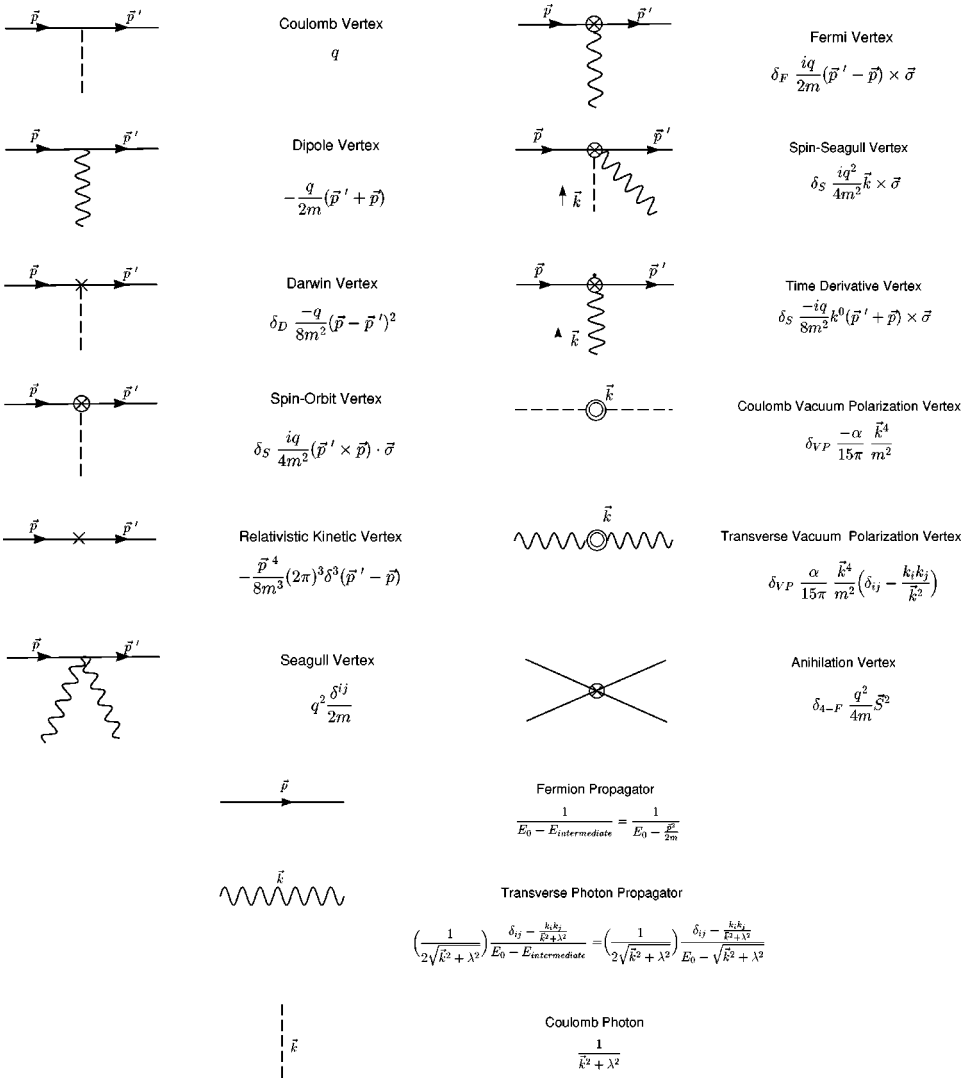

FIG. 1. NRQED Feynman rules.

The Feynman rules for the first few interactions of Eqs. (7), (5) and (6) are given in Fig. 1. We will draw the diagrams with the time flowing to the right. In the rules for the vertices we have followed the example of [6] and used the expression ''dipole vertex'' to represent the $\mathbf{p}\cdot\mathbf{A}$ interaction even though, as pointed out in [6], the NRQED Hamiltonian is not an expansion in multipoles. Also, we have use some Fierz reshuffling to rewrite the annihilation vertex in the form given in Fig. 1. As for the propagators, we have used time ordered perturbation theory where there is one propagator for each different intermediate state, defined by cutting the diagram with a vertical line. The general rule for a time-ordered propagator is

$$\frac{1}{E_0 - E_i} \tag{12}$$

times a factor

$$\frac{1}{2\sqrt{\mathbf{k}^2+\lambda^2}}\left(\delta_{ij} - \frac{k_i k_j}{\mathbf{k}^2+\lambda^2}\right) \tag{13}$$

for each transverse photon present in the intermediate state. In Eq. (12), E_0 stands for the energy of the initial state and E_i for the energy of the intermediate state. One uses nonrelativistic energies, $\mathbf{p}^2/(2m)$, for the fermions and $\sqrt{\mathbf{k}^2+\lambda^2}$ for the photons. In Fig. 1 the propagator is given for an intermediate state containing only one fermion or one transverse photon. In Fig. 2, the corresponding expressions are given for the states containing two fermions or two fermions plus one transverse photons, which are the situations most often met in NRQED calculations.

One must sum over all the possible time ordered diagrams and integrate over all the internal three-momenta, with a measure $d^3p/(2\pi)^3$. Notice that we prefer to include the factors of $1/(2\sqrt{\mathbf{k}^2+\lambda^2})$ corresponding to the transverse photons in the propagators instead of the measure for reasons that will become clearer below.

In this work we will be mainly interested in applications of NRQED to bound state calculations in which case the external lines are not associated with free spinors, but with wave functions. In general, the wave functions are obtained by solving a Bethe-Salpeter type equation, with some ap-

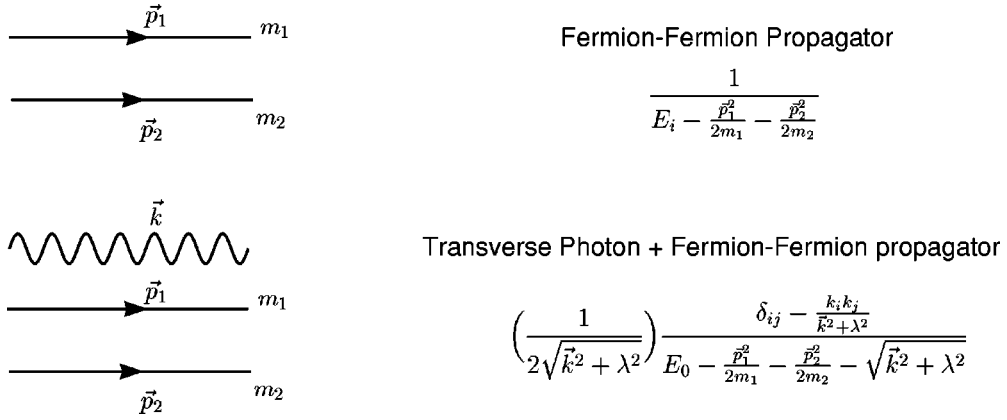

FIG. 2. Time-ordered propagators for two fermions or two fermions plus one transverse photon.

proximated kernel. This is equivalent to summing up an infinite number of this kernel into the wave functions. We will show below that the NRQED counting rules single out (in the Coulomb gauge) the Coulomb interaction as being the only nonperturbative interaction in a nonrelativistic bound state so that this part of the analysis reduces to solving the usual Schrödinger equation. In our explicit examples, we will use the ground state wave function, given by

$$\Psi(\mathbf{p})_{n,l=0,s1,s2}=\frac{8\sqrt{\pi\gamma^5}}{(\mathbf{p}^2+\gamma^2)^2}\otimes\xi_1\otimes\xi_2 \tag{14}$$

where $\gamma\equiv Z\mu\alpha$ [the energy of the state is given by $-\gamma^2/(2\mu)$] and ξ_1,ξ_2 are the spinors of the two particles making up the bound state, with

$$\xi_{up}=\begin{pmatrix}1\\0\end{pmatrix},\quad \xi_{down}=\begin{pmatrix}0\\1\end{pmatrix}. \tag{15}$$

We will not write down the states of higher angular momentum since they are, for the purposes of establishing the counting rules, equivalent to the above states (for the momentum Schrödinger wave functions for arbitrary quantum numbers, see [11]). As just mentioned, using Schrödinger wave functions for the external states means that we are summing the Coulomb interaction between the external legs. All other interactions can be treated perturbatively, which will be shown to be self-consistent with the counting rules.

III. COUNTING RULES: SOFT PHOTONS

We now consider a nonrelativistic bound state made, to simplify the discussion, of two particles of equal masses and of charges $\pm e$. We will also assume that it is in its ground state ($n=1$). We will generalize our results at the end of this section.

There are two important energy scales in such a bound state, the typical bound state momentum γ and the binding energy $-\gamma^2/m$. For a nonrelativistic fermion, for which the dispersion relation is given by the usual $E=\mathbf{p}^2/(2m)$, using either scale leads to $p_{fermion}\approx\gamma$ (from now on, by p and k we will always mean the magnitude of three-momenta). In the case of a photon, for which $E=k$, using the bound state momentum or binding energy yields two very different scales for k, namely $k\simeq\gamma=m\alpha$ and $k\simeq\gamma^2/m=m\alpha^2$. We will refer to this first type of photons as ''soft'' photons, and to the second type as ''ultra-soft'' photons. For the sake of completeness, we define ''hard photons'' as the photons with $k\simeq m$ or greater. These photons play no dynamical role in NRQED, since they have been integrated out of the theory and their only effect is buried in the theory's coefficients.

The first step in deriving counting rules is to separate diagrams involving soft photons from diagrams with ultra-soft photons, since they bring in very different scales, which will necessarily complicate the rules. This is where the use of the Coulomb gauge in conjunction with time ordered PT will be crucial in simplifying the analysis.

Consider a transverse photon exchange between two fermions in a nonrelativistic bound state. This is represented by the two time ordered diagrams of Fig. 3, where we put the time axis toward the right and the Ψ attached to the external lines represent the wave functions. The photon will contain both soft and ultra-soft components. Now, if the photon is soft, its momentum as well as its energy are of order the fermion momentum $m\alpha$ so that its energy is much greater than the fermion energies. This means that from the point of view of the fermions, the propagation of the soft photons is instantaneous and is therefore represented by vertical lines in time-ordered diagrams.

This can be seen more qualitatively by looking at the explicit expression for the intermediate state propagator, which is given by (recall that $k\equiv\sqrt{|\mathbf{k}^2|}$)

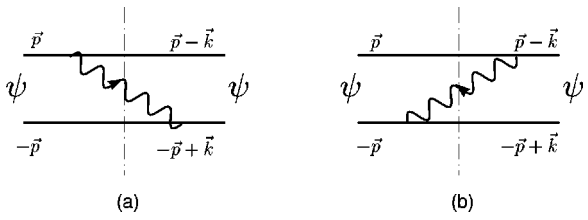

FIG. 3. The two time-ordered diagrams corresponding to the exchange of a transverse photon (the vertical lines indicate the intermediate states used for the time-ordered propagators).

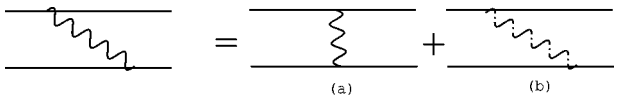

FIG. 4. Separation of a transverse photon into a soft, instantaneous contribution (represented by a vertical line) and an ultra-soft propagator (represented by the broken wavy line).

$$\frac{1}{2k}\left(\delta_{ij}-\frac{k_i k_j}{\mathbf{k}^2}\right)\left(\frac{1}{-\gamma^2/(m)-\mathbf{p}^2/(2m)-(\mathbf{p}-\mathbf{k})^2/(2m)-k}+\frac{1}{-\gamma^2/(m)-\mathbf{p}^2/(2m)-(\mathbf{p}-\mathbf{k})^2/(2m)-k}\right). \tag{16}$$

Notice that the photon mass can be set to zero in bound states calculations, the size of the atom preventing the appearance of any infrared singularity; the scale of the fermion three-momentum $\mathbf{p}$ is of order γ. For soft photons, $k \simeq Z\mu\alpha$, and we clearly see that k dominates in the propagators for the intermediate state so that we can approximate Eq. (18) by

$$\frac{1}{2k}\left(\delta_{ij}-\frac{k_i k_j}{\mathbf{k}^2}\right)\left(\frac{-2}{k}\right)=-\frac{1}{\mathbf{k}^2}\left(\delta_{ij}-\frac{k_i k_j}{\mathbf{k}^2+\lambda^2}\right) \tag{17}$$

which corresponds to a single diagram, with an energy independent photon propagator. This corresponds to the transverse photon propagator of [6] if one approximates $k_0^2-\mathbf{k}^2 \approx -\mathbf{k}^2$ and set $\lambda=0$ [this is why we kept the $1/(2k)$ factor in the definition of the propagator instead of the measure]. This shows again that in a time ordered diagram, the propagation of such a photon is represented by a vertical line, i.e., an instantaneous interaction, since it is independent of k_0 so that its Fourier transform contains a delta function in time.

We can now isolate the soft from the ultra-soft components in any photon exchange by rewriting the time ordered diagram as a sum over an instantaneous interaction and a ''retarded'' one, as in Fig. 4 (this is why we refer to the effects of ultra-soft photons as ''retardation effects''). If we restrict ourselves to NRQED diagrams containing soft photons only, then all photon exchanges can be represented by vertical lines. In real space, such interactions are represented by potentials local in time, i.e., functions of $|\mathbf{r}_1-\mathbf{r}_2|$ only.

Besides photon exchanges, the only other possible interactions are the self-energy interactions such as $-p^4/8m^3$ and the contact interactions contained in $\mathcal{L}_{4-Fermi}$, $\mathcal{L}_{6-Fermi}$, etc. These can clearly be represented by potentials, so that an arbitrary diagram containing soft photons only can be written as a string of potentials connected by fermion lines only. In this case, the intermediate states contain fermion lines only and the time ordered propagators take on a particularly simple form. If there are no interaction from $\mathcal{L}_{n>4}$, for example, the propagators are all of the form

$$\frac{1}{E_0-E(\text{intermediate state})}=\frac{1}{-\gamma^2/m-\mathbf{p}^2/(2m)-\mathbf{p}^2/(2m)}=-\frac{m}{\gamma^2+\mathbf{p}^2} \tag{18}$$

where we have used the fact that the bound state energy is $-\gamma^2/m$. The crucial observation is that the mass dependence factors out, in the form of the overall factor of m, leaving γ as the only dynamical scale in the integrals. If interactions contained in $\mathcal{L}_{n>4}$ are included, then some intermediate states will contain more than two fermion lines, but it will always be of the form

$$\frac{1}{-\gamma^2/m-\Sigma_i \mathbf{p}_i^2/(2m)}=-\frac{m}{\gamma^2+\Sigma_i \mathbf{p}_i^2} \tag{19}$$

and the mass still factors out. Therefore any NRQED diagram containing only soft photons leads to an integral of the form

$$m^b(\Pi_j c_j(\Lambda_R))\int^{\Lambda_R}(\Pi_i d^3p_i)F(\mathbf{p}_i,\gamma) \tag{20}$$

where b is some integer that depends on the types and number of potentials. The product is over all the vertices of type j, with coefficients c_j, as given in Eq. (11). Again, the crucial point for the following discussion is that the mass m does not appear in the integrand, i.e., does not play any dynamical role. There are two scales in the integral, γ and Λ_R, but the invariance under the renormalization group implies that the divergent Λ_R dependent terms arising from the integrations will be canceled by corresponding terms in the bare coefficients $c_i(\Lambda_R)$. As noted before, these divergent terms are either power-law, i.e., of the form $(\Lambda_R)^n$ with n being a positive integer, or logarithmic. The power law terms are canceled exactly whereas the Λ_R in the logarithms get canceled after combining logarithms containing different scales which leaves, in the end, logarithms of α.[1]

How the logarithms become finite is instructive in that it clearly illustrates the separation of scales accomplished by the effective theory. As mentioned in Sec. III, some NRQED bare coefficients contain divergent logarithms of the form $\ln(\Lambda_R/m)$ [as is explicit in Eq. (10)]. To be precise, the NRQED scattering diagrams appearing in the matching process contain logarithms of Λ_R over λ since these are the only two dynamical scales of the eft, whereas the QED scattering diagrams contain logs of the form $\ln(m/\lambda)$; upon solving for the bare coefficients, the logarithmic dependence is then of the form $\ln(\Lambda_R/m)$ (again, the photon mass dependence drops out entirely for the reasons explained above). On the other hand, the NRQED bound state integrals can only depend on the scales Λ_R and γ, yielding $\ln(\Lambda_R/\gamma)$. In the end, the logs

[1]Obviously, dimensional regularization can be used instead of a momentum cutoff. The power law divergences are then either entirely absent or replaced by $1/\epsilon$ divergences. Again, these divergences cancel, by invariance under the renormalization group. This leaves logarithms depending on the scale μ, which gets canceled in the way described above for the $\log \Lambda_R$ terms. In actual explicit analytical calculations, using dimensional regularization or a momentum cutoff is simply a matter of taste. However, for high precision calculations, where numerical calculations are required, an explicit cutoff is necessary.

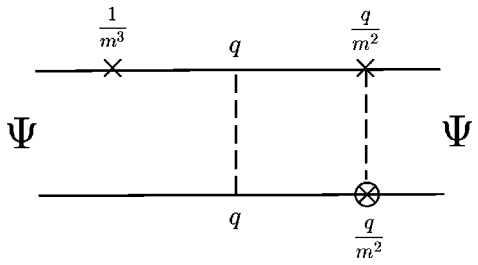

FIG. 5. Generic bound state potential; the dependence on the charges and on the masses of each vertex is indicated.

of the bare coefficients combine with the logs generated by the bound state integrals to give corrections of the form $\ln(\gamma/m)=\ln\alpha$. We see how the use of an effective theory has separated the contributions from all the scales present in the problem (λ, γ, m and Λ_R) in such a way that only two of them played a dynamical role in any given stage of the calculation (λ and m appear in the QED scattering diagrams, Λ_R and λ in the NRQED scattering diagrams, and γ and Λ_R in the NRQED bound state diagrams).

The only Λ_R dependence remaining is therefore of the form $(\gamma/\Lambda_R)^n$ which, upon setting $\Lambda_R=m$, leads to corrections beyond the order of interest; in analytical calculations one can get rid of these terms by simply letting $\Lambda_R\to\infty$ at the end of the calculation, as in conventional renormalization.

It is now a trivial matter to write down the counting rules for an arbitrary bound state diagram containing only soft photons, i.e., the order in α at which it will contribute. There are two sources of factors of α. First, there are the explicit factors contained in the NRQED vertices. Secondly, there is a factor of α for each factor of γ generated by the diagram. To be more rigorous, the factors associated to the vertices are genuine factors of the coupling constant whereas the factors of γ are associated with factors of v which scale is set by the bound state to be of order α; here it is not important to distinguish between the two types of contributions, but this is necessary in QCD bound states because of the noticeable running of the strong coupling constant [12].

By simple dimensional analysis, there will be a factor of γ to compensate each explicit factor of mass appearing in the vertices and each factor of mass due to the fermion pair time ordered propagators. An arbitrary bound state diagram is built out of a given number of potentials, $N_{\mathcal{P}}$, connected by N_{TOP} time ordered propagators. For example, consider Fig. 5, where 3 potentials are connected by 2 time-ordered propagators so that $N_{\mathcal{P}}=3$ and $N_{TOP}=2$ for that diagram. For later use, we also define $\mathcal{V}_i$ as the number of vertices contained in the ith potential and $\mathcal{V}$ as the total number of vertices in the diagram

$$\mathcal{V}=\sum_{i=1}^{N_{\mathcal{P}}}\mathcal{V}_i. \tag{21}$$

We now define the ''vertex mass degree'' d_j as the number of *inverse* masses contained in the jth vertex and the ''potential mass degree'' $\mathcal{D}_i$ as the number of inverse masses contained in the ith potential,

$$\mathcal{D}_i=\sum_{j=1}^{\mathcal{V}_i} d_j. \tag{22}$$

For example, the first potential of Fig. 5 (the self-energy potential) has $\mathcal{D}_1=3$, whereas $\mathcal{D}_2=0$ (for the Coulomb interaction) and $\mathcal{D}_3=4$. Since each potential generates $\mathcal{D}_i$ factors of inverses masses and each fermion-fermion time ordered propagator generates one factor of m, an arbitrary diagram having the dimensions of energy will then generate a factor γ^λ, with

$$\lambda=1-N_{TOP}+\sum_{i=1}^{\mathcal{V}} d_i \tag{23}$$

where the sum is over all the vertices in the diagram. For the present purposes, it is more convenient to write λ as

$$\lambda=1-N_{TOP}+\sum_{i=1}^{N_{\mathcal{P}}}\mathcal{D}_i \tag{24}$$

where now the sum is over all the potentials in the diagram.

We now define the ''coupling constant degree'' $\mathcal{C}_i$ as the total number of explicit factors of α contained in each potential, namely

$$\mathcal{C}_i\equiv\sum_{j}^{\mathcal{V}_i}(n_j+l_j) \tag{25}$$

where n_j and l_j are the powers of α associated with the coefficient of each vertex as defined in Eq. (11).

Finally, a diagram made of $N_{\mathcal{P}}$ potentials will contribute to order $m\alpha^\zeta$ with ζ being the sum of Eq. (24) and the coupling constant degrees (25) of all the potentials:

$$\zeta=\sum_{i=1}^{N_{\mathcal{P}}}(\mathcal{D}_i+\mathcal{C}_i)+1-N_{TOP}. \tag{26}$$

It is easy to see that N_{TOP} and $N_{\mathcal{P}}$ are related by $N_{TOP}=N_{\mathcal{P}}-1$ so that we can write

$$\zeta=\sum_{i=1}^{N_{\mathcal{P}}}(\mathcal{D}_i+\mathcal{C}_i)+2-N_{\mathcal{P}}=\sum_{i=1}^{N_{\mathcal{P}}}(\mathcal{D}_i+\mathcal{C}_i-1)+2. \tag{27}$$

This expression gives the order in α of any NRQED diagram containing only soft photons, keeping in mind that this result can be enhanced by factors of $\ln(\alpha)$. For the example of Fig. 5, one finds $\zeta=8$.

Equation (27) shows clearly that if there is a potential for which $\mathcal{D}_i+\mathcal{C}_i=1$, perturbation theory will break down and it will have to be summed up to infinity. It is an easy matter to find such a potential. We can choose $l_j=0$ (i.e., the coefficients of the vertices have their tree level values). Now, n_j is zero for the self-energy interactions, but the lowest value that the mass degree can take is 3, corresponding to the interaction $-p^4/(8m^3)$, so that the condition $\mathcal{D}_i+\mathcal{C}_i=1$ cannot be fulfilled. Many potentials have $n_j=1$ (i.e., one factor of α) but the only one with, in addition, $\mathcal{D}_i=0$ (no inverse masses) is the Coulomb potential $-e^2/\mathbf{k}^2$. Therefore, as expected,

only the Coulomb interaction must be summed up to infinity and the resulting contribution is, from Eq. (27), of order $m\alpha^2$; all other potentials can be treated in perturbation theory.

In an actual calculation, the counting rules are used in the following way. For a given process (hyperfine splitting, decay rate, etc.), one selects all the diagrams with the appropriate quantum numbers that will, using the counting rules, contribute to the order of interest. The counting rules determine not only the diagrams that must be retained, but also, via the l_j dependence in Eq. (27), the number of loops that must be used in the matching of each vertex. The matching is then carried for each vertex using scattering diagrams in both QED and NRQED. For a given number of loops, there are an infinite number of NRQED scattering diagrams, but here the counting rules are used a second time to pick the NRQED diagrams that need to be taken into account. Notice that in the matching process, which involves scattering diagrams, one uses Eq. (27) even though this relation was derived for bound state diagrams. Once all the relevant diagrams have been taken into account and the NRQED coefficients have been renormalized to the appropriate order, the final calculation will be finite and will reproduce the QED result, to the order of interest.

A. Extension to arbitrary masses and charges

We now extend our counting rules for two constituents having arbitrary masses m_1 and m_2. The above derivation must then be modified at two points. First, the NRQED coefficients given by Eq. (11) will now contain a dependence on m_1 and m_2:

$$c_i(\Lambda_R,m_1,m_2) = c_i^0(m_1,m_2)\alpha^{n_i}\left(1+\sum_{l_i=1}^{\infty}\alpha^{l_i}\tilde{c}_i^{l_i}(\Lambda_R,m_1,m_2)\right). \tag{28}$$

No simple general expression can be given for the mass dependence of the coefficients $\tilde{c}$; it arises from QED loop diagrams entering the matching and may involve logarithms of m_1/m_2, etc. The mass dependence of the zeroth order coefficients c_i^0 can be taken into account in the following way: first, define the vertex mass degrees with respect to each mass, $d_j(m_1)$ and $d_j(m_2)$ as the number of inverse masses m_1 and m_2 contained in the vertex. For a given NRQED bound state diagram, one can then define the following two indices

$$\kappa \equiv \sum_{i=1}^{\mathcal{V}} d_i(m_1), \tag{29}$$

$$\rho \equiv \sum_{i=1}^{\mathcal{V}} d_i(m_2). \tag{30}$$

Obviously, such a diagram will contribute an overall factor $1/(m_1^{\kappa}m_2^{\rho})$. Since the overall result must have the dimensions of energy and since the only energy scale provided by the bound state NRQED diagrams is γ, which contains the reduced mass μ, the overall mass factor will be

$$\frac{\mu^{\kappa+\rho+1}}{m_1^{\kappa}m_2^{\rho}}. \tag{31}$$

The more general counting rule is therefore

$$\mathcal{O} = \frac{\mu^{\kappa+\rho+1}}{m_1^{\kappa}m_2^{\rho}}\alpha^{\zeta} \tag{32}$$

times possible factors of $\ln \mu\alpha$ and functions of the masses m_1, m_2 and μ (which, however, arise only if some of the NRQED coefficients have been matched beyond tree level).

Finally, we consider a bound state with constituents of charges $-e$ and Ze. We first include a Z dependence in the NRQED coefficients:

$$c_i(\Lambda_R,m_1,m_2,) = c_i^0(m_1,m_2)Z^{a_i}\alpha^{n_i} \times\left(1+\sum_{l_i=1}^{\infty}\alpha^{l_i}\tilde{c}_i^{l_i}(\Lambda_R,m_1,m_2,Z)\right) \tag{33}$$

where a_i will denote the explicit power of Z contained in the zeroth order coefficient of the ith vertex. Again, the Z dependence of the $\tilde{c}_i^{l_i}$ arises from the computation of QED loop diagrams and we will not write a general expression for this dependence, but notice that it will necessarily be some power of Z. There is an additional Z dependence which, this time, we can take into account: an additional Z dependence comes from each factor of $\gamma = Z\mu\alpha$ generated by the NRQED bound states. This number is given by Eq. (23):

$$\lambda = 1 - N_{TOP} + \sum_{i=1}^{\mathcal{V}} d_i. \tag{34}$$

A bound state diagram (with all the NRQED coefficients taking their tree level value) will therefore generate a factor Z^{η} with η given by this last expression plus the Z dependence of the tree level NRQED coefficients, as given in Eq. (35):

$$\eta = 1 - N_{TOP} + \sum_{i=1}^{\mathcal{V}} (d_i + a_i). \tag{35}$$

Again, the power of Z is independent of the order in perturbation theory for the Coulomb interaction since each Coulomb potential increases both the sum over a_i and N_{TOP} by one. Our most general counting rule for diagram containing soft photons is therefore given by

$$\mathcal{O} = \frac{\mu^{\kappa+\rho+1}}{m_1^{\kappa}m_2^{\rho}}Z^{\eta}\alpha^{\zeta} \tag{36}$$

times possible factors of $\ln(Z\mu\alpha)$, and dependence on m_1, m_2, μ and Z arising from the loop corrections to the NRQED coefficients.

IV. COUNTING RULES: ULTRA-SOFT PHOTONS

The above derivation relied heavily on the fact that the only scale present in the bound state diagram was γ. However, if we start considering ultra-soft transverse photons, then we have to go back to the general time ordered propagator (see Fig. 3)

$$-\frac{\mathcal{P}_{ij}}{2k}\left(\frac{1}{\gamma^2/(2\mu)+(\mathbf{p}-\mathbf{k})^2/(2m_1)+\mathbf{p}^2/(2m_2)+k}+\frac{1}{\gamma^2/(2\mu)+\mathbf{p}^2/(2m_1)+(\mathbf{p}-\mathbf{k})^2/(2m_2)+k}\right) \tag{37}$$

where we have defined the transverse projection operator

$$\mathcal{P}_{ij}\equiv\delta_{ij}-\frac{k_ik_j}{\mathbf{k}^2}. \tag{38}$$

In general, such a propagator would contain both the soft and ultra-soft scales so that counting rules would be impossible to establish. However, we have already isolated the soft contribution in an instantaneous interaction with the photon propagator given by Eq. (17). Therefore, if the contribution from the soft photon is calculated separately, only the ultra-soft scale remains in Eq. (37). We represent this separation graphically in Fig. 4 where a general transverse photon (on the left-hand side) is represented by a slanted wavy line and, on the right-hand side, the soft photon contribution is represented by a vertical (instantaneous) wavy line and the ultra-soft contribution is represented by a slanted, broken, wavy line. To get the ultra-soft propagator, we must therefore subtract from the general propagator the expression corresponding to the soft photon propagator which we have seen in Eq. (17) to be $-\mathcal{P}_{ij}/\mathbf{k}^2$ (notice, however, that we would not operate this subtraction in a diagram like Fig. 6 where there is no corresponding soft photon contribution):

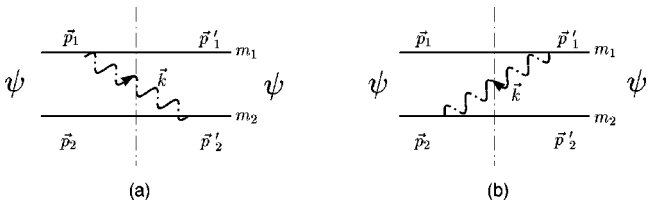

FIG. 6. Ultra-soft photon spanning a Coulomb interaction. In such a diagram, one does not subtract the soft photon propagator from the intermediate state propagator because there is no corresponding soft photon diagram.

$$-\frac{\mathcal{P}_{ij}}{2k}\left(\frac{1}{\gamma^2/(2\mu)+(\mathbf{p}-\mathbf{k})^2/(2m_1)+\mathbf{p}^2/(2m_2)+k}+\frac{1}{\gamma^2/(2\mu)+\mathbf{p}^2/(2m_1)+(\mathbf{p}-\mathbf{k})^2/(2m_2)+k}-\frac{2}{k}\right). \tag{39}$$

This expression now corresponds to the propagator of an ultra-soft photon so the scale of k is of order $\mu\alpha^2$. Recalling that the scale of p is $\simeq\mu\alpha$, we can perform a Taylor expansion in $k/p\simeq\alpha$. Applying this to Eq. (39) gives

$$\approx-\frac{1}{2k}\,\mathcal{P}_{ij}\left(\frac{1}{\gamma^2/(2\mu)+\mathbf{p}^2/(2\mu)+k}-\frac{1}{k}+\frac{\mathbf{p}\cdot\mathbf{k}/m_1}{(\gamma^2/(2\mu)+\mathbf{p}^2/(2\mu)+k)^2}\right. \tag{40}$$

$$+\frac{-\mathbf{k}^2/(2m_1)}{(\gamma^2/(2\mu)+\mathbf{p}^2/(2\mu)+k)^2}+\frac{(\mathbf{p}\cdot\mathbf{k})^2/m_1^2}{(\gamma^2/(2\mu)+\mathbf{p}^2/(2\mu)+k)^3} \tag{41}$$

$$\left.+\frac{-\mathbf{k}^2\mathbf{p}\cdot\mathbf{k}/m_1^2}{(\gamma^2/(2\mu)+\mathbf{p}^2/(2\mu)+k)^3}+\frac{(\mathbf{k}\cdot\mathbf{p})^3/m_1^3+}{(\gamma^2/(2\mu)+\mathbf{p}^2/(2\mu)+k)^4}+\cdots\right)+\text{same with } m_1\leftrightarrow m_2 \tag{42}$$

where the first line contain the zeroth order term plus the first order one (the $\mathbf{p}\cdot\mathbf{k}$ term), the second line contains the second order contribution and so on.

Since the expansion is in k/p, we expect that each power of $\mathbf{k}$ appearing in the numerator will be associated with a power of α with respect to the zeroth order term of the Taylor expansion [the first term in Eq. (40)]. We will show this explicitly for a few terms.

Consider first the zeroth order propagator. It contains two inverse powers of k, which scales like $\mu\alpha^2$, so that it contributes to the counting rules by a factor $1/(m^2\alpha^4)$ (we will not distinguish between m_1, m_2 and μ to discuss the counting rules). Of course, in an actual diagram, other factors will enter to make the overall α contribution of the diagram positive; here we are just interested in the relative contribution of the terms in the Taylor expansion.

Now consider the first order correction [the second term of Eq. (42)]. The numerator $\mathbf{k}\cdot\mathbf{p}/m$ scales like $m\alpha^2$

$\times m\alpha/m = m\alpha^3$ and the denominator contains 3 factors of k so it scales like $(m\alpha^2)^3$. Therefore, the first order propagator scales like

$$m\alpha^3/(m^3\alpha^6) = 1/(m^2\alpha^3) \tag{43}$$

which is one power of α times the zeroth order propagator. The $\mathbf{k}^2/m$ term in the second order Taylor propagator (41) scales like

$$(m\alpha^2)^2/(m\times m^3\alpha^6) = 1/(m\alpha)^2 \tag{44}$$

which is down by two powers of α with respect to the zeroth order propagator. It is a simple matter to verify that the other term of Eq. (41) also contribute with a factor of α^2 with respect to the lowest order contribution, and the terms of Eq. (42) contribute with a factor α^3, etc.

In an actual diagram, the Taylor expansion must of course be carried on the whole diagram. As an illustration, we expand the complete integrand corresponding to Fig. 3(a), sandwiched between ground state wave functions:

$$\begin{aligned}
&\frac{8\sqrt{\pi\gamma^5}}{(\mathbf{p}^2+\gamma^2)^2}\frac{q_1q_2}{4m_1m_2}(2p_i-k_i)(k_j-2p_j)\frac{\mathcal{P}_{ij}}{2k}\left(\frac{1}{-\gamma^2/(2\mu)-(\mathbf{p}-\mathbf{k})^2/(2m_1)-\mathbf{p}^2/(2m_2)-k}+\frac{1}{k}\right)\frac{8\sqrt{\pi\gamma^5}}{((\mathbf{p}-\mathbf{k})^2+\gamma^2)^2}\\
&\quad=\frac{(8\sqrt{\pi\gamma^5})^2}{(\mathbf{p}^2+\gamma^2)^4}\frac{q_1q_2}{4m_1m_2}\frac{\mathcal{P}_{ij}}{2k}\frac{4p_ip_j\mathbf{p}\cdot\mathbf{k}/m_1}{(-\gamma^2/(2\mu)-\mathbf{p}^2/(2\mu)-k)^2}+\frac{(8\sqrt{\pi\gamma^5})^2}{(\mathbf{p}^2+\gamma^2)^4}\frac{q_1q_2}{4m_1m_2}\frac{\mathcal{P}_{ij}}{2k}\\
&\quad\times\left(\frac{1}{(-\gamma^2/(2\mu)-\mathbf{p}^2/(2\mu)-k)}+\frac{1}{k}\right)\left(-4p_ip_j+2k_ip_j+2p_ik_j-\frac{16p_ip_j\mathbf{p}\cdot\mathbf{k}}{(\mathbf{p}^2+\gamma^2)}+\cdots\right).
\end{aligned} \tag{45}$$

Again, one can easily verify that each power of $\mathbf{k}$ in the numerator is associated with an extra factor of α.

Notice that the spin-spin diagram with an ultra-soft photon, Fig. 7(b), contains at least two powers of $\mathbf{k}$ since the NRQED Feynman rule for the Fermi vertex is proportional to $\mathbf{k}$; in other words, the first non-vanishing contribution comes from the second order term in the Taylor expansion. Therefore, the lowest order contribution of the ultra-soft spin-spin exchange is suppressed by two powers of α with respect to the corresponding dipole-dipole exchange (this is due to the fact that the Fermi interaction involves the $\mathbf{B}$ field). This is very different from the corresponding soft photon diagrams which both contribute to the same order. The difference, again, is that only the factors of e and $1/m$ enter in the soft photon counting rules whereas factors of the photon momentum $\mathbf{k}$ matter in the ultra-soft counting rules.

Clearly, the fact that one power of α is generated by each term in the Taylor expansion will prove crucial in writing down the counting rules of this new, Taylor expanded, version of NRQED. However, before doing so, we now want to show that the Taylor expansion we just carried is equivalent to a multipole expansion of the NRQED vertices.

A. Connection with the multipole expansion

As an example, consider the $-q\psi^\dagger(\mathbf{p}\cdot\mathbf{A}+\mathbf{A}\cdot\mathbf{p})/(2m)\psi$ interaction contained in the term $-\psi^\dagger\mathbf{D}^2/(2m)\psi$ in the Hamiltonian. To obtain the NRQED Feynman rule, we first expand the fields in plane waves:

$$+qi\left(\frac{e^{-i\mathbf{p}'\cdot\mathbf{r}}\boldsymbol{\nabla}\cdot\boldsymbol{\epsilon}(e^{-i\mathbf{k}\cdot\mathbf{r}}e^{i\mathbf{p}\cdot\mathbf{r}})}{2m}+\frac{e^{-i\mathbf{p}'\cdot\mathbf{r}}(e^{-i\mathbf{k}\cdot\mathbf{r}}\boldsymbol{\epsilon}\cdot\boldsymbol{\nabla}e^{i\mathbf{p}\cdot\mathbf{r}})}{2m}\right) \tag{46}$$

where $\mathbf{p},\mathbf{p}'$ are, respectively, the three momenta of the fermion line before and after the interaction, and $\mathbf{k}$ is the photon three-momentum; $\boldsymbol{\epsilon}$ is the photon polarization. Applying the derivatives, we get

$$\frac{q}{2m}(k_i-2p_i)e^{-i(\mathbf{p}'+\mathbf{k}-\mathbf{p})\cdot\mathbf{r}}. \tag{47}$$

The exponential leads, as usual, to the conservation of three-momentum $\mathbf{p}'=\mathbf{p}-\mathbf{k}$ (here we considered a photon being emitted). Using this to write $-2\mathbf{p}=-\mathbf{p}-\mathbf{p}'-\mathbf{k}$ and discarding all factors associated with the external fields, we obtain the Feynman rule

$$-q\frac{p_i+p_i'}{2m}. \tag{48}$$

The rule is obviously unchanged if we consider an absorbed photon. Now we consider a multipole expansion of this vertex, i.e., we expand the photon field

$$e^{-i\mathbf{k}\cdot\mathbf{r}}=1-i\mathbf{k}\cdot\mathbf{r}+\tfrac{1}{2}(-i\mathbf{k}\cdot\mathbf{r})^2+\cdots. \tag{49}$$

In the following, we will use the notation $e^{-i\mathbf{k}\cdot\mathbf{r}}$ = zeroth order + first order + $\cdots$ to label the terms in the multipole expansion. As usual, this expansion makes sense only if $kr\ll 1$. The size of r is set by the bound state to be of order

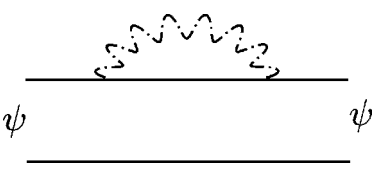

FIG. 7. Spin-spin exchange with a soft photon (vertical line) and an ultra-soft photon.

the Bohr radius $r \simeq 1/\gamma$. For ultra-soft photons, we have $k \simeq \gamma^2/\mu$ so that $kr \simeq \alpha$ and the multipole expansion is valid. Of course, it would be nonsensical to use it for soft photons. Also, the multipole expansion is clearly the same as the Taylor expansion performed above since the scale of $r \simeq 1/p$.

We can easily find the rule for the new vertex. Using the first term of the multipole expansion, $e^{-i\mathbf{k}\cdot\mathbf{r}}=1$ (corresponding to an E1 transition) in Eq. (46), we obtain

$$-\frac{p_i}{m}e^{-i(\mathbf{p}'-\mathbf{p})\cdot\mathbf{r}} \tag{50}$$

where now the exponential leads to the condition $\mathbf{p}'=\mathbf{p}$, i.e., three momentum is *not* conserved at the vertices when the multipole expansion is used. This can, however, still be used to write the rule for the vertex as before, i.e.,

$$-q\frac{p_i+p_i'}{2m}. \tag{51}$$

Even though the rule for the vertex is the same as before, the condition $\mathbf{p}'=\mathbf{p}$ simplifies greatly the expression for diagrams containing ultra-soft photons and, in particular, the propagator. To see this, we first go back to the time ordered photon-fermion pair propagator (39). We now use in addition the fact that the fermion momenta at the vertices are unchanged by the emission or absorption of the photon to write Eq. (39) as

$$-\frac{\mathcal{P}_{ij}}{2k}\left(\frac{1}{\gamma^2/(2\mu)+\mathbf{p}^2/(2\mu)+k}+\frac{1}{\gamma^2/(\mu)+\mathbf{p}^2/(2\mu)+k}-\frac{2}{k}\right)$$
$$=-\frac{\mathcal{P}_{ij}}{k}\left(\frac{1}{\gamma^2/(2\mu)+\mathbf{p}^2/(2\mu)+k}-\frac{1}{k}\right) \tag{52}$$

instead of the form (39) which was obtained by using $\mathbf{p}'=\mathbf{p}-\mathbf{k}$. In Eq. (52), the scale of k is set either by $\gamma^2/(2\mu) \simeq \mu\alpha^2$ or $\mathbf{p}^2/(2\mu)$, but since $\mathbf{p}$ is a fermion three-momentum it is of order γ, we get in either case $k \simeq \mu\alpha^2$. This shows explicitly that the multipole expansion has permitted us to isolate the ultra-soft scale.

To obtain the higher order terms in the multipole expansion, one provides a factor $(\pm\mathbf{k}\cdot\boldsymbol{\nabla}_{\mathbf{p}})^n/n!$ for each vertex connected to an ultra-soft photon, where n is the order of interest in the multipole expansion, and a plus (minus) sign is used if the photon is absorbed (emitted). In this expression, the gradient must be taken with respect to the three-momentum of the fermion line on the *right* of the vertex. To apply these rules, it is therefore necessary to distinguish between the momentum of the fermion before and after the interaction, even though we have to set them equal in the end.

To illustrate this, we will evaluate the first few multipole corrections to the ultra-soft photon propagator. Since, as noted above, one must distinguish the momenta of each fermion and the momenta before and after the interaction, we will use the momenta as labeled in Fig. 8, with the understanding that one must set

$$\mathbf{p}_1=\mathbf{p}_1'=-\mathbf{p}_2=-\mathbf{p}_2'=\mathbf{p} \tag{53}$$

after carrying out the derivatives. Taking this into account, the intermediate state propagator in Fig. 8(a) is

$$-\frac{1}{2k}\,\mathcal{P}_{ij}\left(\frac{1}{k+\gamma_2/(2\mu)+\mathbf{p}_1'^2/(2m_1)+\mathbf{p}_2^2/(2m_2)}-\frac{1}{k}\right) \tag{54}$$

and the propagator of Fig. 8(b) is

$$-\frac{1}{2k}\,\mathcal{P}_{ij}\left(\frac{1}{k+\gamma_2/(2\mu)+\mathbf{p}_1^2/(2m_1)+\mathbf{p}_2'^2/(2m_2)}-\frac{1}{k}\right). \tag{55}$$

If we consider Fig. 8(a), then we only have to consider the multipole expansion of the vertex on the upper line since the other vertex will not act on the intermediate state propagator. We therefore apply, as we did above, the operator $-\mathbf{k}\cdot\boldsymbol{\nabla}_{\mathbf{p}_1'}$ on Eq. (54) to obtain

$$\frac{\mathcal{P}_{ij}}{2k}\,\frac{-\mathbf{k}\cdot\mathbf{p}/m_1}{[k+\gamma_2/(2\mu)+\mathbf{p}^2/(2\mu)]^2}. \tag{56}$$

In the case of Fig. 8(b), we apply the operator $i\mathbf{k}\cdot\boldsymbol{\nabla}_{\mathbf{p}_2'}$ on Eq. (55) with, for result (recall that we replace $\mathbf{p}_2$ by $-\mathbf{p}$ after differentiating)

$$-\frac{\mathcal{P}_{ij}}{2k}\,\frac{\mathbf{k}\cdot\mathbf{p}/m_2}{[k+\gamma^2/(2\mu)+\mathbf{p}^2/(2\mu)]^2}. \tag{57}$$

As expected, this is the same as Eq. (56) with m_2 replaced by m_1. The sum of Eqs. (56) and (57) is the result of the first order term of the multipole expansion. To be more precise, this is the result obtained from considering the first order term in the multipole expansion of either vertex.

The result of the second order multipole can easily be calculated in a similar way. We apply the operator $(-\mathbf{k}\cdot\boldsymbol{\nabla}_{\mathbf{p}_1'})^2/2$ to Eq. (54) and $(\mathbf{k}\cdot\boldsymbol{\nabla}_{\mathbf{p}_2'})^2/2$ to Eq. (55) to obtain

$$\frac{\mathcal{P}_{ij}}{2k}\left(\frac{\mathbf{k}^2/(2m_1)}{[k+\gamma^2/(2\mu)+\mathbf{p}^2/(2\mu)]^2}-\frac{(\mathbf{k}\cdot\mathbf{p})^2/m_1^2}{[k+\gamma^2/(2\mu)+\mathbf{p}^2/(2\mu)]^3}+\text{same with } m_2\to m_1\right). \tag{58}$$

These expressions correspond to keeping the $n=2$ multipole term on either of the vertices plus the first order term on both vertex, all of which contribute to the same order in α, as we will discuss in the next section.

We also give the third order result:

$$\frac{\mathcal{P}_{ij}}{2k}\left(\frac{\mathbf{k}^2\mathbf{k}\cdot\mathbf{p}/m_1^2}{[k+\gamma^2/(2\mu)+\mathbf{p}^2/(2\mu)]^3}-\frac{(\mathbf{k}\cdot\mathbf{p})^3/m_1^3}{[k+\gamma^2/(2\mu)+\mathbf{p}^2/(2\mu)]^4}+\text{same with } m_2\to m_1\right). \tag{59}$$

We have recovered the expressions obtained from the Taylor expansion, Eqs. (40), (41) and (42). This is not surprising since the Taylor expansion of a function $f(x+a)$ around $x=0$ can be written as

$$f(x+a)_{x\simeq 0}=e^{xd/da}f(a) \tag{60}$$

and this is what the multipole expansion accomplishes.

In an actual calculation, the multipole expansion must of course be carried on the whole diagram. This is slightly more complex because the wave functions must also be written in a way that distinguishes the momenta on each fermion line. To illustrate this, we consider again the bound state diagram corresponding to Fig. 8(a) and work out the expression in first order of the multipole expansion. We again use the ground state wave function (14) for the external states. Taking this into account, the integrand corresponding to Fig. 8(a) is given by

$$\frac{8\sqrt{\pi\gamma^5}}{\mu^2(\mathbf{p}_1^2/m_1+\mathbf{p}_2^2/m_2+\gamma^2/\mu)^2}\frac{q_1q_2}{4m_1m_2}(\mathbf{p}_1+\mathbf{p}_1')_i(\mathbf{p}_2+\mathbf{p}_2')_j\frac{\mathcal{P}_{ij}}{2k}$$
$$\times\left(\frac{1}{-\gamma^2/(2\mu)-\mathbf{p}_1'^2/(2m_1)-\mathbf{p}_2^2/(2m_2)-k}+\frac{1}{k}\right)\frac{8\sqrt{\pi\gamma^5}}{\mu^2(\mathbf{p}_1'^2/m_1+\mathbf{p}_2'^2/m_2+\gamma^2/\mu)^2}. \tag{61}$$

The contribution of the zeroth order in the multipole expansion is obtained by simply using the relations (53) directly in Eq. (61). The contribution of the first order multipole expansion is then obtained by applying on this expression the operator $-\mathbf{k}\cdot\boldsymbol{\nabla}_{\mathbf{p}_1'}$, which is associated with the vertex on the left in Fig. 8(a) plus the operator $\mathbf{k}\cdot\boldsymbol{\nabla}_{\mathbf{p}_2'}$ for the second vertex, and then reexpressing the vectors in terms of $\mathbf{p}$ using Eq. (53). The result is

$$\frac{q_1q_2}{4m_1m_2}\frac{8\sqrt{\pi\gamma^5})^2}{(\gamma^2+\mathbf{p}^2)^4}\frac{\mathcal{P}_{ij}}{2k}\left(\frac{4\mathbf{p}_i\mathbf{p}_j\mathbf{k}\cdot\mathbf{p}/m_1}{[-\gamma^2/(2\mu)-\mathbf{p}^2/(2\mu)-k]^2}\right)$$
$$+\frac{q_1q_2}{4m_1m_2}\frac{8\sqrt{\pi\gamma^5})^2}{(\gamma^2+\mathbf{p}^2)^4}\frac{\mathcal{P}_{ij}}{2k}$$
$$\times\left(\frac{1}{-\gamma^2/(2\mu)-\mathbf{p}^2/(2\mu)-k}+\frac{1}{k}\right)$$
$$\times\left(2\mathbf{k}_i\mathbf{p}_j+2\mathbf{k}_j\mathbf{p}_i-16\mathbf{p}_i\mathbf{p}_j\frac{\mathbf{k}\cdot\mathbf{p}}{(\mathbf{p}^2+\gamma^2)}\right). \tag{62}$$

This is, as expected, equal to the expression obtained from the first order Taylor expansion (45). A similar calculation for Fig. 8(b) gives the same result as Eq. (62) with $m_1\leftrightarrow m_2$.

Notice that the zeroth order term in the multipole expansion is obtained by setting $\mathbf{p}'=\mathbf{p}$ in the NRQED vertices. In the case of the Fermi vertex, this gives zero since the NRQED Feynman rule is proportional to $\mathbf{p}'-\mathbf{p}=\mathbf{k}$. This means that the first nonzero contribution is of the first order in the multipole expansion. Higher order terms are obtained as above, i.e., by applying the corresponding factor of $(\pm\mathbf{k}\cdot\boldsymbol{\nabla}_{\mathbf{p}})^n/n!$.

Even though we have simply recovered the expressions obtained by performing a simple Taylor expansion, there is one important reward for doing so: one can use directly the Wigner-Eckart theorem and the familiar selection rules derived in quantum mechanics for each interaction generated by the Taylor expansion. This has consequences in decays of positronium, and in nonrelativistic QCD bound states [12].

To summarize, we have seen that, starting from NRQED, separating the soft and ultra-soft scales and applying a multipole expansion to (or Taylor expanding) the vertices con-

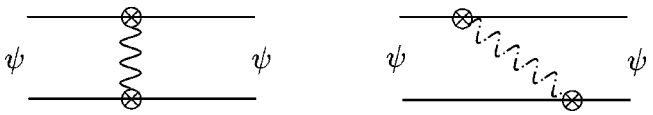

FIG. 8. The two time-ordered diagrams corresponding to a transverse photon exchange with the routing necessary to apply the multipole expansion.

nected to ultra-soft photons generates an extension of NRQED with its own set of Feynman rules. This theory, which we will call ''MQED'' (for ''Multipole QED'') has the advantage of generating bound state diagrams that contribute to a unique order in α. In the last section, we will derive the MQED Feynman rules and show some applications of the counting rules.

V. MQED COUNTING RULES

We can now easily extend the counting rules to include diagrams containing ultra-soft photons. The concept of potentials is not well-defined, however, when ultra-soft photons are present, so we first rewrite the soft counting rule (26) as a sum over vertices instead of a sum over potentials:

$$\zeta(\text{soft photons}) = \sum_{j=1}^{N_\mathcal{V}} (d_j + n_j + l_j) + 1 - N_{TOP} \tag{63}$$

where $N_\mathcal{V}$ is the total number of vertices contained in the diagram. For a diagram containing ultra-soft photons, this rule must be changed to

$$\zeta(\text{ultra-soft photons}) = \sum_{j=1}^{N_\mathcal{V}} (d_j + n_j + l_j) + 1 - N_{TOP} + 2N_\gamma + \mathcal{M}_{ultra\text{-}soft} \tag{64}$$

where N_γ is the number of ultra-soft photons in the diagram. The origin of the $2N_\gamma$ term can be understood in the following way: each ultra-soft photon brings in a factor $\int d^3k/(2k)$ which scales as $(m\alpha^2)^2$ (once the multipole expansion has been applied). This must be divided by the square of a scale having the dimensions of energy, but since the only remaining scale, after integration of the ultra-soft photons, is γ, the final result is $(m\alpha^2)^2/(m\alpha)^2 = \alpha^2$. Therefore, each ultra-soft photon leads to two additional powers of α in the counting rules, hence the factor $2N_\gamma$ in Eq. (64).

Notice that each time-ordered propagator decreases the power of α by one, no matter whether the intermediate state contains ultra-soft photons or not. We have already shown this when ultra-soft photons are absent (in which case the intermediate states contain only fermions). In the presence of a single ultra-soft photon, the intermediate state propagator takes the form (we take, for simplicity, $m_1 = m_2$)

$$\frac{1}{-\gamma^2/m - \mathbf{p}^2/m - k} \tag{65}$$

which scales as $1/(m\alpha^2)$. Once again, after integration over the photon momentum, the only remaining scale to yield the correct dimension is γ, hence a correction of order $(m\alpha)/(m\alpha^2) = 1/\alpha$ for each time-ordered propagator containing an ultra-soft photon. This result can easily be extended to diagrams containing any number of ultra-soft photons. Recall that the same result was obtained in absence of ultra-soft photons, but for very different reasons. There, the factor of mass could be factored out of the propagator since no photon three-momentum k appeared in the denominator, and this factor of m was divided by a factor of γ, leaving a factor $m/\gamma = 1/\alpha$.

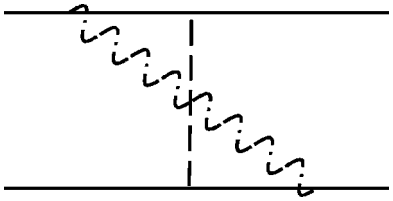

FIG. 9. Self-energy diagram with an ultra-soft photon.

The last term of Eq. (64), $\mathcal{M}_{ultra\text{-}soft}$ can be expressed in two different ways, depending on whether one uses a Taylor expansion of the diagram or a multipole expansion of the vertices. In the first case, $\mathcal{M}_{ultra\text{-}soft}$ is simply the power of $\mathbf{k}$ appearing in the numerator. In the second case, $\mathcal{M}_{ultra\text{-}soft}$ can be written as

$$\mathcal{M}_{ultra\text{-}soft} = \sum_i \mathcal{M}_i \tag{66}$$

where the sum is over the vertices connected to ultra-soft photon and $\mathcal{M}_i$ is the order in the multipole expansion to which the ith vertex has been expanded.

Equation (66) gives the order, in powers of α, at which an arbitrary MQED diagram will contribute. The dependence on arbitrary masses is unchanged by the presence of ultra-soft photons and is therefore still given by Eq. (32). The charge dependence, however, is different when there are ultra-soft photons because the ultra-soft scale is $\simeq \gamma^2/\mu \simeq \mu Z^2\alpha^2$ so that the Z dependence is different than in the soft scale $\gamma = Z\mu\alpha$. The expression for the charge dependence must then be changed from Eq. (35) to

$$\eta = 1 - N_{TOP} + \sum_{i=1}^{\mathcal{V}} (d_i + a_i) + 2N_\gamma + \sum_{\mathcal{V}_i} \mathcal{M}_i \tag{67}$$

where, again, the last sum is over the vertices connected to ultra-soft photons only.

Our final result is therefore that an arbitrary MQED diagram will contribute to order

$$\mathcal{O} = \frac{\mu^{\kappa+\rho+1}}{m_1^\kappa m_2^\rho} Z^\eta \alpha^\zeta \tag{68}$$

with ζ defined in Eq. (64), η defined in Eq. (67) and κ and ρ defined in Eq. (30).

We now give a few examples of the use of Eq. (68). As a first example consider the interaction Fig. 9 in hydrogen, where the ultra-soft photon is connected to an electron line. In this diagram, $d_1 = d_2 = 1$ (there is one factor of $1/m$ on each vertex), $n_1 = n_2 = 1/2$ (a factor e on each vertex), $l_1 = l_2 = 0$ (the $\mathbf{p}\cdot\mathbf{A}$ interaction does not get renormalized), $N_{TOP} = 1$, $N_\gamma = 1$ and, if the zeroth order in the multipole expansion (or in the Taylor expansion) is used, $\mathcal{M}_1 = \mathcal{M}_2 = 0$. This leads to a contribution of order α^5. The mass de-

pendence is found to be μ^3/m_e^2 and the Z dependence is, from Eq. (67), Z^4. This diagram therefore contributes to order

$$\frac{\mu^3 Z^4}{m_e^2}\alpha^5. \tag{69}$$

In fact, this result is enhanced by a logarithm $\ln(Z\alpha)$ and contributes to the Lamb shift.

Consider now Fig. 7(a) in positronium so that $Z=1$ and $m_1=m_2=m_e$. In this diagram, the transverse photon is soft (it is represented by a vertical line). We can therefore use Eq. (63), i.e., the counting rules for soft photons. One has $n_1=n_2=1/2$ and $d_1=d_2=1$. If the tree level expressions are used for the coefficients, then this diagram contributes to order $m_e\alpha^4$. The same diagram will contribute to higher order in α if the loop corrections to the coefficients of the Fermi vertices are considered [the one-loop correction being, from Eq. (10), $\alpha/2\pi$].

As a final example, consider Fig. 7(b). Here the photon is ultra-soft. As mentioned previously, the first nonvanishing contribution from this diagram contains two factors of **k** (one from each spin vertex) so that $\mathcal{M}_{ultra\text{-}soft}$ in Eq. (64) is at least equal to two. $N_{TOP}=1$, $N_\gamma=1$ and the other coefficients are as in Fig. 7(a), if the tree level coefficients are used. One then finds that this diagram will contribute to order $m_e\alpha^7$.

Let us conclude by comparing this paper to recent, closely related, work by other authors. First, a new effective field theory containing only ultrasoft photons, pNRQED (for ''potential NRQED'') has been developed by Pineda and Soto [13]. Let us say that MQED is not equivalent to pNRQED in the sense that MQED is not a new ultra-soft effective field theory, independent of NRQED. Our derivation is much closer in spirit to the recent work of Beneke and Smirnov [14], in which they consider the threshold expansion of loop diagrams in relativistic quantum field theories. They show how to extract the contributions due to different scales, without having to resort to an effective field theory approach. This is similar to the present work in the sense that we extract the ultrasoft contributions from the NRQED integrals without constructing any new effective field theory. Let us mention that Beneke and Smirnov identify, in addition to the soft and ultrasoft scales described in the present paper (their ''potential'' scale corresponds to our ''soft scale''), an additional low energy scale. The connection of this additional scale with MQED will be explored in a future publication.

ACKNOWLEDGMENTS

I have benefited from many useful conversations with Peter Lepage who suggested first the idea of applying the multipole expansion to NRQED. I also want to thank S. M. Zebarjad for several very useful comments and M. Beneke for discussions concerning [14]. I have benefited from the hospitality of the CERN theory division during part of this work. This work was supported by NSERC (Canada), and by les fonds FCAR du Québec.

[1] C. Itzykson and J.-B. Zuber, *Quantum Field Theory* (McGraw-Hill, New York, 1980).
[2] M. H. L. Pryce, Proc. R. Soc. London **B195**, 62 (1948); S. Tani and Soryushiron Kenkyu **1**, 15 (1949) (in Japanese); Prog. Theor. Phys. **6**, 267 (1951); L. L. Foldy and S. A. Wouthuysen, Phys. Rev. **78**, 29 (1950).
[3] W. E. Caswell and G. P. Lepage, Phys. Rev. A **20**, 36 (1979).
[4] T. Kinoshita and G. P. Lepage, in *Quantum Electrodynamics*, edited by T. Kinoshita (World Scientific, Singapore, 1990), pp. 81–89.
[5] P. Labelle, G. P. Lepage, and U. Magnea, Phys. Rev. Lett. **72**, 2006 (1994).
[6] M. Nio and T. Kinoshita, Phys. Rev. D **53**, 4909 (1996).
[7] P. Labelle and S. M. Zebarjad, hep-ph/9611313.
[8] P. Labelle, Ph.D. thesis, Cornell University, 1994.
[9] C. P. Burgess and David London, Phys. Rev. Lett. **69**, 3428 (1992).
[10] P. Labelle, in Proceedings of the 14th MRST Meeting, Toronto, Ontario, 1992, edited by P. J. O'Donnell, hep-ph/9209266.
[11] B. Podolsky and L. Pauling, Phys. Rev. **34**, 109 (1929).
[12] G. T. Bodwin, E. Braaten, and G. P. Lepage, Phys. Rev. D **51**, 1125 (1995).
[13] A. Pineda and J. Soto, Nucl. Phys. B (Proc. Suppl.) **64**, 428 (1998); Phys. Lett. B **420**, 391 (1998); Phys. Rev. D (to be published), hep-ph/9802365; hep-ph/9805424.
[14] M. Beneke and V. A. Smirnov, Nucl. Phys. **B522**, 321 (1998).